J Solid State Electrochem (2005) 9: 380–389
DOI 10.1007/s10008-004-0635-5

ORIGINAL PAPER

Antje Widmann · Heike Kahlert · Harm Wulff
Fritz Scholz

Electrochemical and mechanochemical formation of solid solutions of potassium copper(II)/zinc(II) hexacyanocobaltate(III)/ hexacyanoferrate(III) $KCu_xZn_{1-x}[hcc]_x[hcf]_{1-x}$

Received: 28 September 2004 / Revised: 13 October 2004 / Accepted: 12 November 2004 / Published online: 12 May 2005

Abstract Electrochemical reduction/oxidation cycles of immobilised powder mixtures of KCu[hcc] and KZn[hcf] as well as their mechanical milling lead to the formation of a quaternary solid solution (mixed crystals) with Cu^{2+} and Zn^{2+} on the nitrogen coordinated sites and Fe^{3+} and Co^{3+} on the carbon coordinated sites. The reaction products were studied by the X-ray diffractometry and voltammetric techniques. The formation of solid solutions of the general formula $KCu_xZn_{1-x}[hcc]_x[hcf]_{1-x}$ is the first example of an electrochemical and mechanochemical reaction leading to mixed hexacyanometalates.

Keywords Tribochemistry · Cyclic voltammetry · XRD · Hexacyanoferrates · Solid solutions

Introduction

Transition metal hexacyanometalates form a class of zeolitic inorganic compounds that have been studied extensively because of their outstanding properties. These compounds show reversible insertion electrochemistry [1–4], electrochromism [5–11], the capability to be used in rechargeable batteries [12–16] and possess electrocatalytic activities [17–20]. Potassium zinc(II) hexacyanoferrate(II) has been used as ion exchanger [21–24]. Most metal hexacyanometalates belong to the cubic crystal system [25–27]. However, some metal hexacyanometalates have hexagonal crystal structures as, e.g., zinc- and silver hexacyanoferrate(III) [28–30]. For some metal hexacyanometalates it is well known that isomerisation reactions occur during electrochemical conversion, e.g., chromium(II) hexacyanoferrate(III) isomerises to iron(II) hexacyanochromate(III) [31]. It has long been known that iron(II) hexacyanochromate(III) also undergoes thermal isomerisation to chromium(III) hexacyanoferrate(II) at a temperature around 100 °C [32–34]. Several authors have described the synthesis and the electrochemical and magnetic behaviour of substitutional solid solutions of metal hexacyanometalates with substituted nitrogen coordinated metal ions [35–39]. Recently, we have described solid solutions where the carbon coordinated positions are populated by two kinds of metal ions [40] and also mixed solid solutions where both the nitrogen and carbon coordinated sites are populated by two different metal ions. All these solid solutions have been synthesised by precipitation from solutions. Nothing is known about the reactivity of metal hexacyanometalate mixtures with different crystal structures. The formation of solid solutions of such parent systems has not yet been described. Tribochemical reactions have been reported during grinding of metal hexacyanoferrates(III) (*M*[hcf], with *M* being K^+, Zn^{2+}, Mn^{2+}, Co^{2+}, Ni^{2+} and Cu^{2+}, respectively) with KBr. During that reaction the metal hexacyanoferrate(III) is reduced to the metal hexacyanoferrate(II) and Br^- is oxidised to Br_2 [41]. The sequence of reactivity has been found to be $K^+ << Zn^{2+} < Mn^{2+}$, Co^{2+}, $Ni^{2+} < Cu^{2+}$.

The objective of this paper is to report on electrochemical and tribochemical reactions of potassium copper(II) hexacyanocobaltate(III) (KCu[hcc]) with potassium zinc(II) hexacyanoferrate(III) (KZn[hcf]) and to compare the reaction product with a compound synthesised by precipitation. Because the electrochemical properties of hexacyanometalates are very sensitive

Dedicated to Professor Dr. G. Horányi on the occasion of his 70th birthday.

A. Widmann · H. Kahlert (✉) · H. Wulff · F. Scholz
Institut für Chemie und Biochemie,
Universität Greifswald, Soldmannstr. 23,
17489 Greifswald, Germany
Tel.: +49-3834-864452
Fax: +49-3834-864451
E-mail: hkahlert@uni-greifswald.de

and typical fingerprints of the involved compounds [42, 43], the insertion electrochemistry of the starting materials was studied by voltammetry of immobilised particles (VIM) [44–46]. The X-ray diffractometry was also applied as a most suitable tool to study the solid reaction products.

Experimental

Equipment

Electrochemical measurements were performed using an AUTOLAB system with a PGSTAT 20 (Eco-Chemie, Utrecht, The Netherlands) in conjunction with a three-electrode system and a personal computer (IBM compatible). The reference electrode was an Ag/AgCl electrode (3 M KCl) (Metrohm, Herisau, Switzerland) with a potential of 0.208 V versus SHE at 25 °C. A platinum wire served as an auxiliary electrode. Working electrodes used in this study were paraffin-impregnated graphite electrodes (PIGE), prepared from graphite rods (electrodes for spectrographic analysis, VEB Elektrokohle Lichtenberg, Berlin, Germany) impregnated in molten paraffin [44–46]. For all cyclic voltammetric measurements, a scan rate of 50 mV s^{-1} was used.

The diffuse reflectance spectra were measured using a Leitz Laborlux 12 Pol S incident light microscope (Leica Microsystems, Wetzlar, Germany) with two crossed linear polarised filters to minimise the specular reflectance. The microscope was coupled via fibre optics with a transputer-integrated diode array system (TIDAS) (J & N Analytische Meß-und Regeltechnik, Ahlen, Germany) with a spectral range of 400–800 nm and a personal computer (IBM compatible).

The X-ray powder diffraction data were collected at room temperature in parafocusing BRAGG-BRENTANO geometry with a D5000 Siemens diffractometer (Siemens, Germany) equipped with a secondary graphite monochromator. CuK_α radiation was used. The continuous scan was applied in the 2Θ range 10°–90° with 10 s fixed time for each 0.02° per 2Θ step. The quantitative analysis and the calculation of the lattice constants were performed using the Rietveld method (FULLPROF [47, 48]). For all diffraction patterns, the peak profiles were modelled using a pseudo-Voigt function.

The samples were milled with a ball mill Vibrator (Narva, Brand-Erbisdorf, Germany). The diameter of the inner ball was 1 cm and of the outer ball was 2.6 cm.

Electrode preparation

The solid compounds were studied by employing cyclic voltammetry with microparticles attached to the surface of a PIGE (cf. the VIM) [44–46] in 0.1 M KNO_3 solution with a scan rate of 50 mV s^{-1}. The sample preparation was carried out as follows: 1–3 mg of the sample powder were placed on a glass plate. The electrode was gently rubbed over the material in order to immobilise some traces on the electrode surface. After measurement, the electrode surface was cleaned by rubbing over abrasive paper and finally polished on white printing paper.

Chemicals

The chemicals used were all of p.a. quality and purchased from Merck (Germany): $K_3[Fe(CN)_6]$, $CuCl_2$, KNO_3, $CoCl_2{\cdot}6\ H_2O$, KCN, $ZnCl_2$, conc. H_2SO_4 and conc. HCl. Bidistilled water was used throughout. $K_3[Co(CN)_6]$ was synthesised according to [49].

Synthesis of $KCu[hcc]{\cdot}5.7\ H_2O$

A 0.2 mol L^{-1} solution of $K_3[Co(CN)_6]$ was added dropwise to the stirred solution of 0.2 mol L^{-1} solution of $CuCl_2$ with an excess of KNO_3. Following the addition the precipitate was allowed to stand for one night and then centrifuged. After washing twice with bidistilled water, it was dried at 40 °C. The dried product formed a light blue green glassy solid, which was milled in a mortar and washed carefully several times with bidistilled water to remove last traces of potassium nitrate and chloride.

Synthesis of $KZn[hcf]{\cdot}0.25\ H_2O$

A 0.2 mol L^{-1} solution of $K_3[Fe(CN)_6]$ was added dropwise to the stirred solution of 0.2 mol L^{-1} solution of $ZnCl_2$ with an excess of KNO_3. After the addition the precipitate was allowed to stand for one night and then centrifuged. After washing twice with bidistilled water, it was dried at 40 °C. The dried product formed a light-yellow solid. The washing procedure was the same as in the case of $KCu[hcc]{\cdot}5.7\ H_2O$.

Synthesis of $K_{0.4}Cu_{0.65}Zn_{0.65}[hcc]_{0.55}[hcf]_{0.45}{\cdot}6\ H_2O$

The mixed solutions of 0.1 mol L^{-1} $K_3[Co(CN)_6]$ and 0.1 mol L^{-1} $K_3[Fe(CN)_6]$ were added dropwise to the mixed and stirred solution of 0.1 mol L^{-1} $CuCl_2$ and 0.1 mol L^{-1} $ZnCl_2$ with an excess of KNO_3. After addition the precipitate was allowed to stand for one night and then centrifuged. After washing twice with bidistilled water, it was dried at 40 °C. The dried product formed a yellow-brown glassy solid. The washing procedure was the same as in the case of $KCu[hcc]{\cdot}5.7\ H_2O$.

Milling process to form $KCu_xZn_{1-x}[hcc]_x[hcf]_{1-x}$

$KCu[hcc]{\cdot}5.7\ H_2O$ and $KZn[hcf]{\cdot}0.25\ H_2O$ were given in a ratio of 1:1 into a ball mill and milled in 2 min steps.

After each milling step, a sample of the milling product was taken for CV, diffuse reflectance spectroscopy and X-ray measurements. The whole milling process took 2 h.

Milling experiment with dried samples

$KCu[hcc]\cdot 5.7\ H_2O$ and $KZn[hcf]\cdot 0.25\ H_2O$ were dried at 180 °C for about 2 h. The dried compounds were milled in a weight ratio of 1:1 in the ball mill, which was placed in a glove box. The air in the glove box was dried with silica gel before for about 1 week. After milling, the X-ray measurements were done immediately.

Chemical analysis

CHN-analyses were done using LECO-CHNS-932 (Leco, St. Joseph, USA). Before performing AAS analysis, the samples were digested in the following way: 0.25 g of the powder sample were boiled for about 1 h with 20 mL conc. H_2SO_4 and afterwards 20 mL conc. HCl was given to the solution and boiled for another hour. After boiling the solution was given into a 100-mL flask and filled up with bidistilled water. The AAS-measurements were performed using an AAS 3100 (Perkin-Elmer, Rodgau-Jüdesheim, Germany). The evaluation was made by using calibration curves with 1 g L^{-1} standard solutions from Merck (Darmstadt, Germany). The following analytical data have been determined. (a) $K_{0.2}Cu_{1.4}[Co(CN)_6]\cdot 5.7\ H_2O$ (KCu[hcc]):

	Mass (%)						
	K	Cu	Co	C	H	N	O
Found	2.12	21.44	14	17.18	2.2	20.74	22.32
Calculated	1.86	21.14	14.02	17.14	2.73	19.99	23.12

(b) $K_{0.32}Zn_{1.34}[Fe(CN)_6]\cdot 3\ H_2O$ (KZn[hcf]):

	Mass (%)						
	K	Zn	Fe	C	H	N	O
Found	3.55	24.16	15.55	19.71	1.704	23.31	12.02
Calculated	3.42	23.93	15.25	19.68	1.65	22.95	13.12

(c) $K_{0.4}Cu_{0.65}Zn_{0.65}[hcc]_{0.55}[hcf]_{0.45}\cdot 6\ H_2O$:

	Mass (%)								
	K	Cu	Zn	Fe	Co	C	H	N	O
Found	3.44	10	11	5.96	7.68	17.43	2.8	20.94	20.75
Calculated	3.71	9.81	10.10	5.97	7.69	17.11	2.87	19.95	22.79

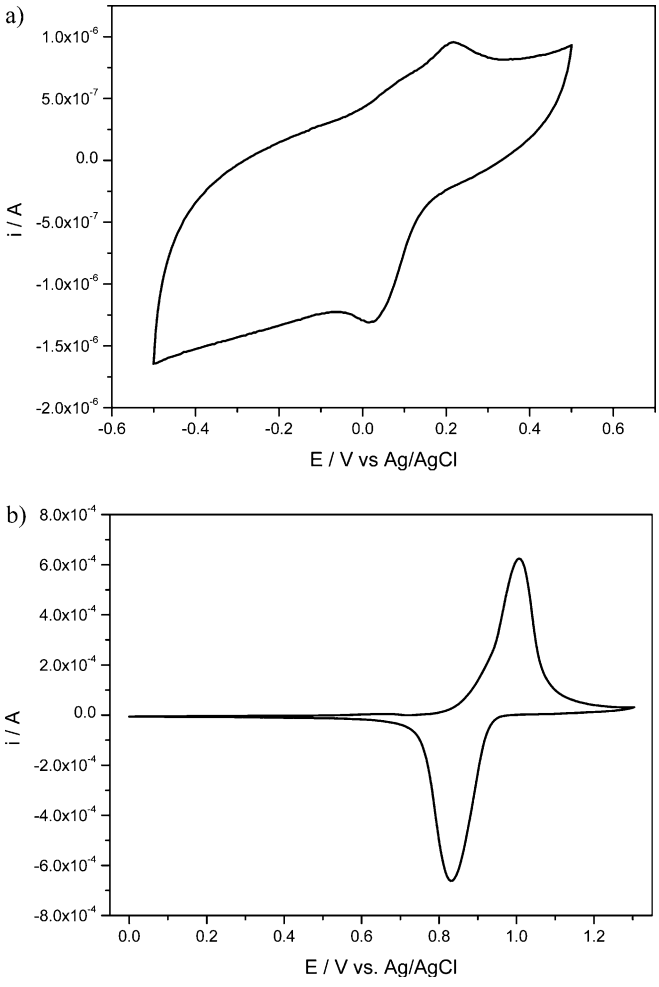

Fig. 1 Cyclic voltammogram of **a** KCu[hcc], **b** KZn[hcf] in 0.1 M KNO_3

Results and discussion

Electrochemical properties

Mechanochemical formation of $KCu_xZn_{1-x}[hcc]_x[hcf]_{1-x}$

Figure 1a shows a cyclic voltammogram of pure KCu[hcc]. As reported earlier, an oxidation/reduction system is obtained at a formal potential of ca. 70 mV versus Ag/AgCl [40]. The mid-peak potential of the cyclic voltammograms is taken as the formal potential of the voltammetric system [47]. This system is caused by the copper(II)/copper(I) reduction/oxidation [50] coupled with the insertion/expulsion of K^+ ions:

$$KCu^{2+}[hcc] + e^- + K^+_{aq} \rightleftarrows K_2Cu^{1+}[hcc]. \quad (1)$$

Figure 1b shows a cyclic voltammogram of pure KZn[hcf]. The peak system at 918 mV is due to the reduction/oxidation of the low-spin iron ions of the hexacyanoferrate units coupled with the insertion/expulsion of K^+ ions:

$$KZn[hcf] + K^{+}_{aq} + e^{-} \rightleftarrows K_2Zn[hcf]. \quad (2)$$

This peak system is reversible and completely stable in cyclic voltammetry. An important feature of the two electrochemical systems is that the peak currents of the copper system (Fig. 1a) are about three orders of magnitudes smaller than the peak currents of the iron system (Fig. 1b). This leads in experiments with powder mixtures of the two compounds to the fact that the copper system is not detectable together with the iron system, although it is present, of course. The reasons for the low currents of KCu^{2+} [hcc] are not clear yet. Surface confinements of the reduction can be excluded from experiments with a chemical reduction of KCu^{2+} [hcc] by ascorbic acid, where complete reduction is observed [40].

An experiment was made in which both solids were milled in a weight ratio of 1:1 and samples were taken in intervals of 1 min at the beginning of the experiment to measure the cyclic voltammograms. At the end of the experiment longer time intervals between the samplings were chosen. It results that by milling over a longer time the iron(II)/iron(III) redox system of KZn[hcf] disappears after some scans. Already after milling for 1 min only the reduction peak disappeared (Fig. 2a) and after milling 5 min the oxidation peak could be found only during the first scan (Fig. 2b). After milling 40 min the oxidation peak of KZn[hcf] can still be found but only during the first scan. A new peak system appears at 637 mV which exhibits stability and reversibility. The peak potentials of both compounds, the starting compound KZn[hcf] and the compound with the new voltammetric system at 637 mV, shift within the time of milling. Figure 3a shows the dependence of the oxidation peak potential of KZn[hcf] on the milling time. The oxidation peak potential shifts by 170 mV to negative values within 50 min of milling. The strongest shift takes place during the first 10 min. Because the reduction peak of the KZn[hcf] cannot be observed, nothing can be said about a shift of the formal potential. The formal potential of the new formed phase definitely shifts during the milling (Fig. 3b). This shift is much smaller than the shift of the oxidation peak potential of KZn[hcf]. A potential shift is typical when a new ''mixed'' compound, i.e. substitutional solid solution is formed [37].

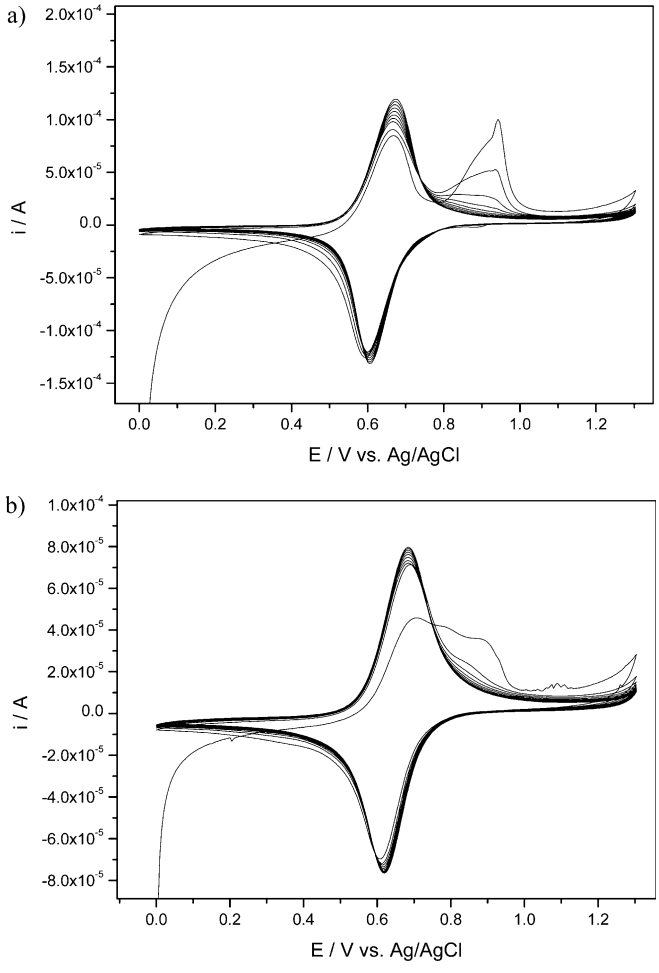

Fig. 2 Cyclic voltammogram of KZn[hcf] mixed with KCu[hcc] in 0.1 M KNO_3, after milling **a** 1 min, **b** 5 min

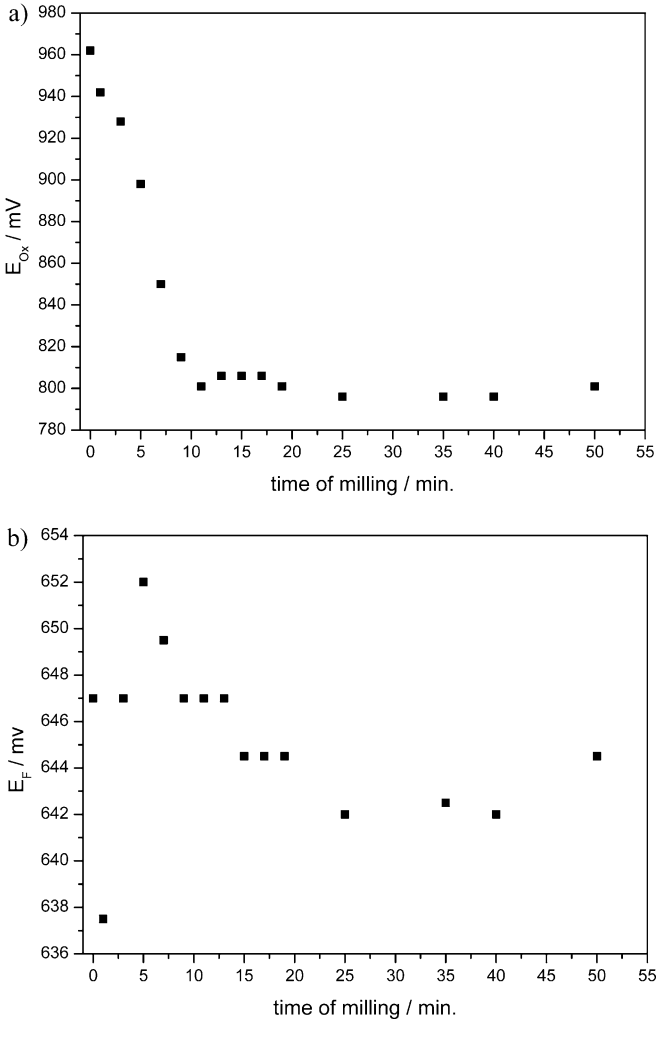

Fig. 3 **a** Dependence of the oxidation peak potential of KZn[hcf] in the time of milling. **b** Dependence of the formal potential of $KCu_xZn_{1-x}[hcc]_x[hcf]_{1-x}$ in the time of milling

The CV experiments allow to suppose that a new substitutional solid solution with the formula $KCu_xZn_{1-x}[hcc]_x[hcf]_{1-x}$ is formed during milling:

$$x\,KCu[hcc] + 1 - x\,KZn[hcf] \rightleftarrows KCu_xZn_{1-x}[hcc]_x[hcf]_{1-x}. \quad (3)$$

Electrochemical formation of $KCu_xZn_{1-x}[hcc]_x[hcf]_{1-x}$

When two solid compounds are immobilised as a mechanical mixture on the surface of an electrode, usually two independent signals are observed [40, 51]. However, when KCu[hcc] and KZn[hcf] were mixed together in a weight ratio of 1:1, a very different observation was made. In the case of this mixture of KCu[hcc] and KZn[hcf], it is not possible to see the copper(II)/copper(I) redox system of KCu[hcc] because the iron(II)/iron(III) system of KZn[hcf] has much higher currents. Interestingly during the first scan, a new peak system appears at a formal potential of 637 mV while the peak system belonging to the iron ions of KZn[hcf] is found at a formal potential of 925.5 mV (Fig. 4a). During the next cycles the iron(II)/iron(III) peak system of KZn[hcf] decreases and after 23 scans it totally disappeared while the new peak system at the formal potential of 637 mV increases and exhibits a small shift of 10 mV into positive direction (end potential = 647 mV) (Fig. 4b, c).

As described in the *Experimental Section*, the compound $K_{0.4}Cu_{0.65}Zn_{0.65}[hcc]_{0.55}[hcf]_{0.45}{\cdot}6\ H_2O$ was synthesised by co-precipitation as a reference substance and the cyclic voltammograms of that compound were recorded. Only one electrochemically active reversible peak system is observed (Fig. 5). After 30 scans the formal potential is 647 mV which is exactly the same formal potential of the compound that formed in the course of milling experiments described above. Because of this fact, the compound $K_{0.4}Cu_{0.65}Zn_{0.65}[hcc]_{0.55}[hcf]_{0.45}{\cdot}6\ H_2O$ can be taken as a reference substance to understand the milling experiments and the cyclic voltammograms of the powder mixtures.

X-ray investigations

Figure 6 shows the powder diffraction patterns of the parent substances (a) KZn[hcf] and (b) KCu[hcc]. The X-ray patterns of the two phases are different due to their different crystal structures. The crystal structure of the Prussian blue analogue sample KCu[hcc] was solved on the basis of the model of Keggin and Miles [25] and is described elsewhere [40]. The space group of KCu[hcc] is $Fm\bar{3}m$. The structure of potassium zinc(II) hexacyanoferrate(III) KZn[hcf] has not yet been described in the literature. LoosNeskovic et al. [29, 30] have reported on the crystal structure of alkali (Na, K) zinc(II) hexacyanoferrate(II), $MZn_{1.5}[hcf]$.

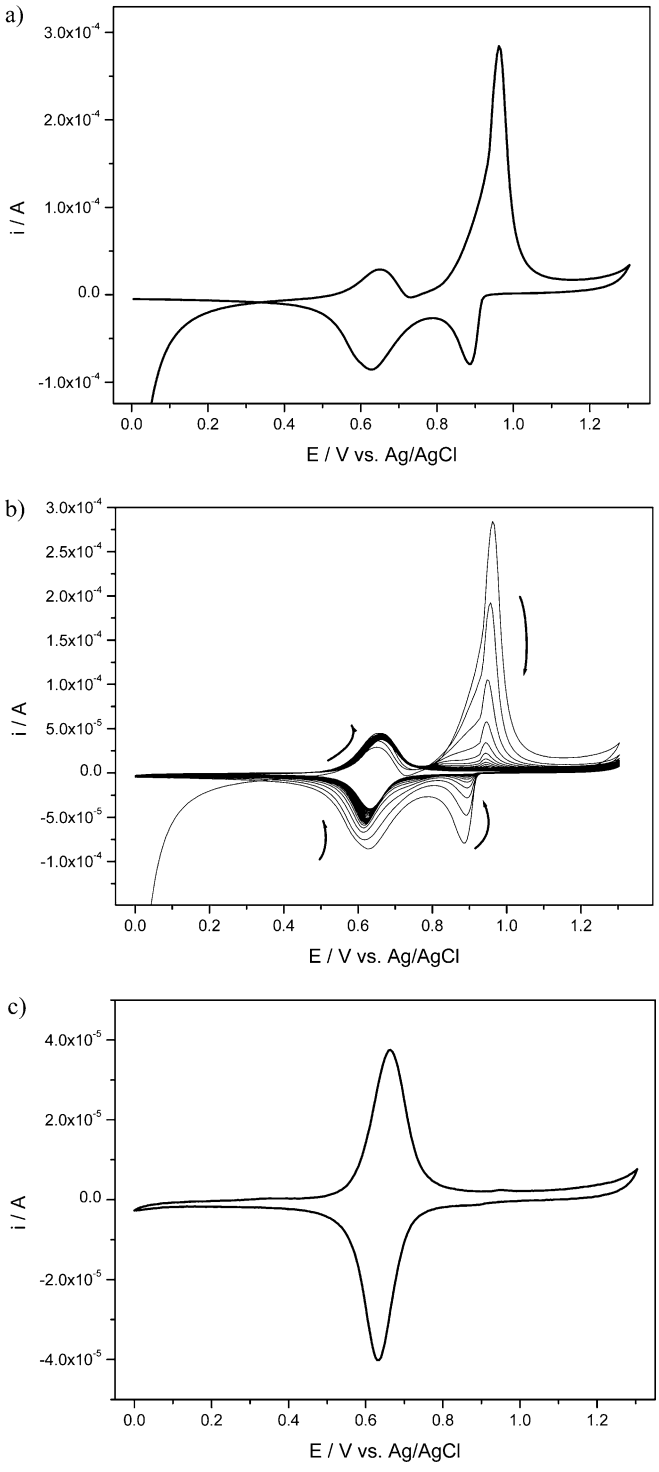

Fig. 4 **a** Cyclic voltammogram of KZn[hcf] mixed with KCu[hcc] in 0.1 M KNO_3, **a** 1.scan, **b** 1.-30. scan, and **c** 30. scan

KZn[hcf] forms a hexagonal lattice $(SG: R\bar{3}c)$. Its X-ray powder pattern looks like the potassium-free zinc(II) hexacyanoferrate(III) [52]. About the structure data of the zinc hexacyanoferrate(III) compounds we will report in a separate paper.

Figure 7a shows the powder pattern of the 1:1 mixture of KZn[hcf] and KCu[hcc] after a milling time of

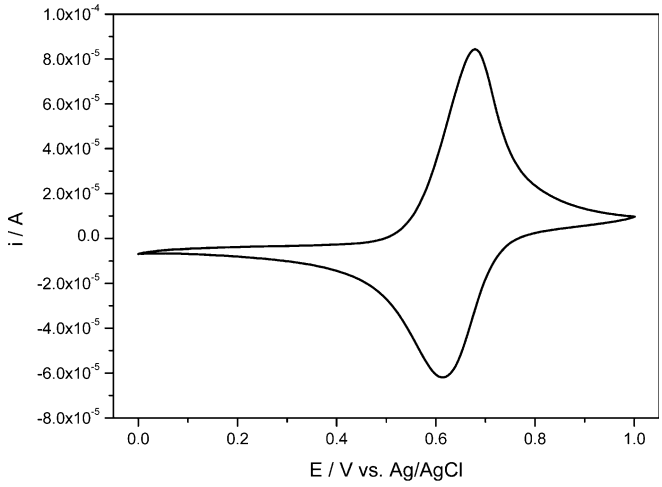

Fig. 5 Cyclic voltammogram of $K_{0.4}Cu_{0.6}Zn_{0.7}[hcc]_{0.55}[hcf]_{0.45}\cdot 6\ H_2O$ in 0.1 M KNO_3, 30. scan

1 min. The patterns of both compounds are clearly observable, but all the peak positions of the cubic KCu[hcc] are shifted to smaller angles. The lattice constants (Fig. 8a) as well as the intensities of the cubic phase and the intensity ratio KCu[hcc]/KZn[hcf] (Fig. 8b) increase linearly up to a milling time of 13 min. Longer milling times cause decreasing peak intensities of both compounds. No further shift of the peak positions could be observed. This behaviour is in very good agreement with electrochemical measurements: CV data also show that KZn[hcf] degrades during the milling process. The degradation can be clearly seen up to 13 min, too. After 45 min the diffraction patterns show only weak and strongly broadened reflections of the cubic phase (Fig. 7b). The crystalline samples become more and more amorphous. The lattice parameters are given in Table 1. To prove whether the resulting compound is a new substitutional solid solution of the composition $KCu_xZn_{1-x}[hcc]_x[hcf]_{1-x}$, X-ray powder diffraction data were collected of the chemically synthesised reference substance $K_{0.4}Cu_{0.65}Zn_{0.65}[hcc]_{0.55}[hcf]_{0.45}\cdot 6\ H_2O$. The X-ray pattern of the reference substance is nearly identical to the pattern of cubic

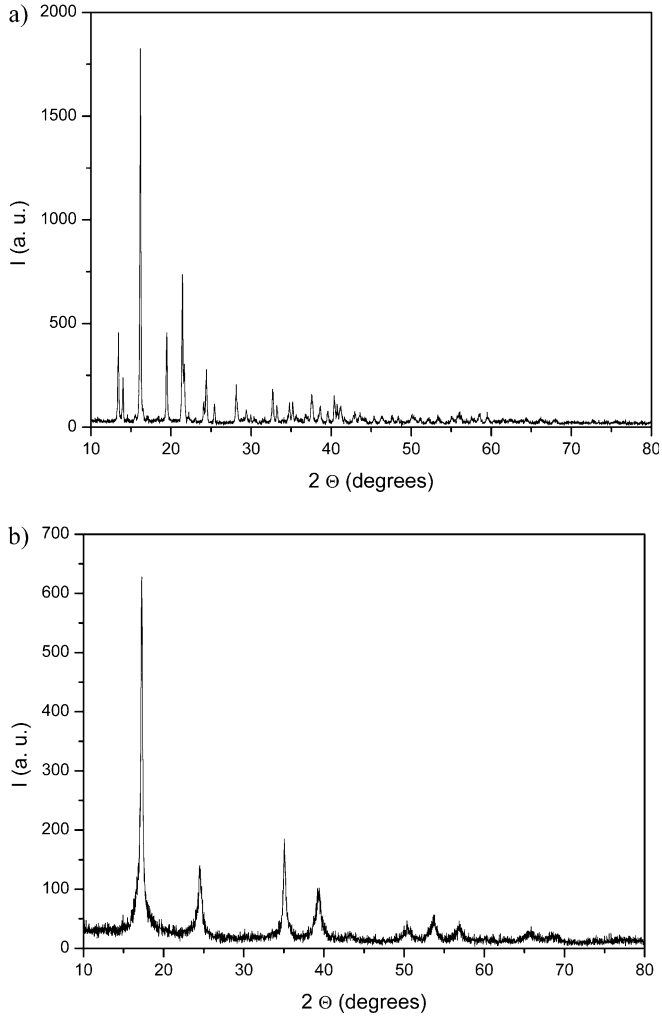

Fig. 6 X-ray powder pattern of **a** KZn[hcf], **b** KCu[hcc]

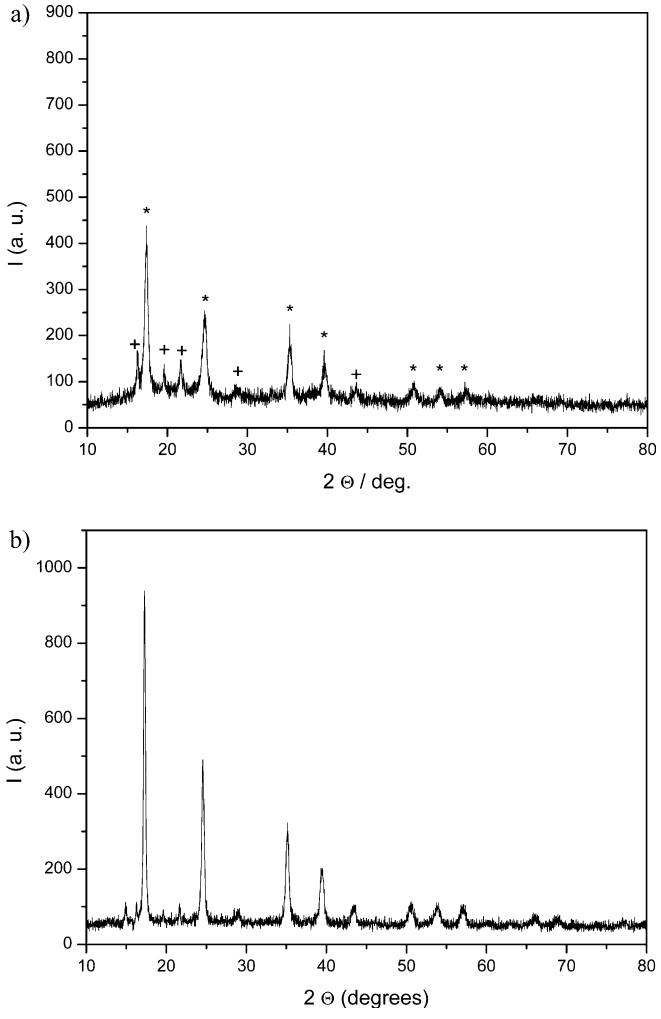

Fig. 7 **a** X-ray powder pattern of the mixture of KZn[hcf] and KCu[hcc] after 13 min milling. *Plus symbol* hexagonal phase, *asterisk* cubic phase. **b** X-ray powder pattern of $K_{0.4}Cu_{0.65}Zn_{0.65}[hcc]_{0.55}[hcf]_{0.45}\cdot 6\ H_2O$

Table 1 Milling time, lattice constants of KCu[hcc], percentage of the mixture components KCu[hcc]/KZn[hcf], Goodness of fit values (R_{wp}/R_{exp}), mean domain sizes (< D >) of KZn[hcf] and of KCu[hcc]

Milling time (min)	Lattice constant (Å)	KCu[hcc]/KZn[hcf] (%)	R_{wp}/R_{exp}	< D > (nm)	
				KCu[hcc]	KZn[hcf]
0	10.043(2)	44/56	6.34/3.72	53	150
1	10.053(2)	49/51	6.62/3.59	46	127
3	10.074(3)	53/47	6.46/3.68	35	86
5	10.100(3)	59/41	6.63/3.59	24	66
7	10.124(4)	63/37	6.83/3.58	22	50
9	10.138(3)	68/32	10.1/3.59	21	39
11	10.144(4)	73/27	11.7/3.66	19	32
13	10.157(3)	80/20	11.9/3.66	20	25
15	10.145(3)	79/21	11.2/3.73		
20	10.142(4)	76/24	12.6/3.89		

The mean domain sizes were calculated using the Scherrer equation. The line profiles were fitted by a pseudo Voigt function. The integral breadths of diffraction line profiles were corrected with the integral breadths of the instrumental function

KCu[hcc]. Differences mainly exist in the peak positions (Fig. 7c).

Rietveld refinements show that the composition of the powder mixture KZn[hcf] and KCu[hcc] changes during the milling process (Fig. 8a) and that the lattice constant of the cubic phase increases within the milling time (Fig. 8b). This observation can only be explained with an introduction of larger ions into the cubic lattice of KCu[hcc]. Zn^{2+} (88 pm) is larger than Cu^{2+} (87 pm). The size difference between the anions may also cause an increase of the lattice constants: Co^{3+} (68.5 pm); $Fe^{3+}{}_{ls}$ (69 pm) [53]. Only the introduction of both, the cations and anions, into the cubic KCu[hcc] can explain the observed expansion of the cubic unit cell.

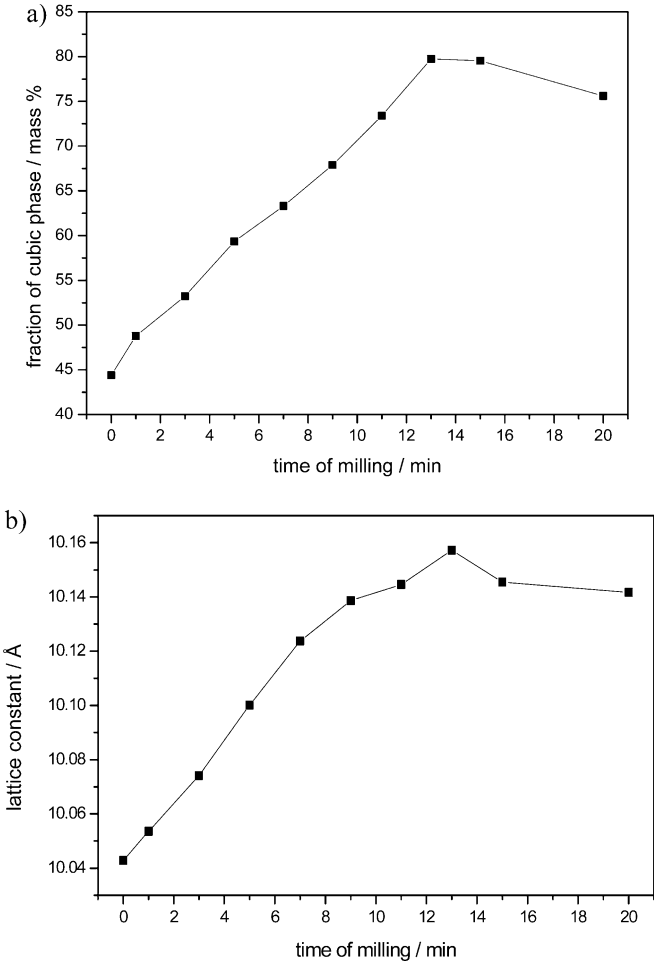

Fig. 8 **a** Fraction of the cubic phase in the powder mixture of KZn[hcf] and KCu[hcc] versus milling time. **b** Lattice constant of the cubic phase versus milling time

To prove whether the crystal water plays an important role in the reaction pathway in this solid state reaction, the samples where dried at 180 °C for 2 h. The DTA/TG-curves showed that at this temperature all water has left the compounds. The X-ray powder patterns of the pure compounds show that the crystal structure remains stable after drying. The same milling experiment as described above was performed with the dried samples. One result of drying was that the compounds were not as stable as before. After 1 min milling of a mixture of both dried samples in a weight ratio 1:1, peak intensities of both compounds decrease. No shift in the peak positions can be observed. The same result occurs after grinding 3 min. After 5 min milling the peaks of both compounds can be found, but most of the mixture is X-ray-amorphous. In contrast to the grinding experiments described above, here both phases disappear and even the cubic phase is yet amorphous after milling of 9 min. The fact that the peaks decrease simultaneously and that there is no peak shift in the cubic phase prove that no solid state reaction takes place. Otherwise the cubic phase should have remained longer stable than the hexagonal phase and a change in the lattice parameters of at least one compound should have been observed.

Diffuse reflectance spectroscopy

The pure KZn[hcf] has a light yellow colour with an absorption band at 425 nm due to charge transfer from the cyanide ligand to iron(III), which is found in the diffuse reflectance spectra transformed into the Kubelka–Munk function. The light blue green KCu[hcc] has a typical absorption band at 711 nm (Fig. 9) due to

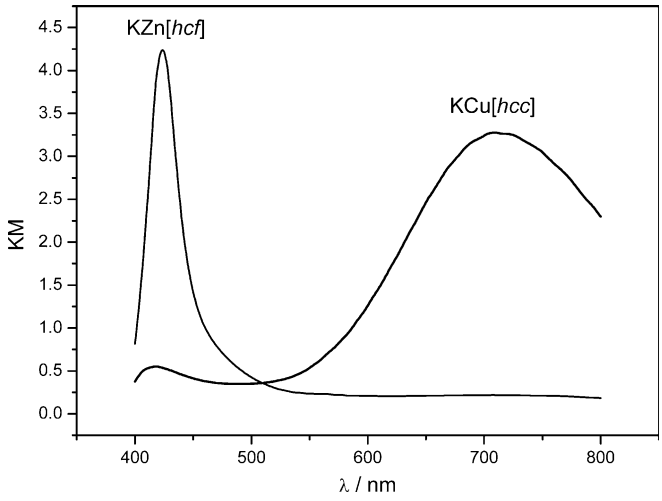

Fig. 9 Diffuse reflectance spectrum transformed into the Kubelka–Munk function of KZn[hcf] and KCu[hcc]

copper(II) ions. The charge transfer from the cyanide ligand to cobalt ions is not visible in the measured range. During the milling, the colour changes from light yellow-green after 1 min milling through dark grey-green (at a milling time of 25 min.) to grey-brown after about 2 h (see Fig. 10). During the milling, the absorption band at 425 nm shifts up to 440 nm and the intensity increases within the time of milling. The second absorption band shifts from 761 nm to 768 nm and the intensities increase with milling time. After milling for about 2 h, a new absorption band appears at around 550 nm. This band is associated with the iron to copper charge transfer in cupric ferricyanide [54].

Mechanism

A schematic mechanism for the reaction of KCu[hcc] with KZn[hcf] is proposed and discussed on the basis of the results of electrochemistry and the X-ray investigations. Figure 11a shows schematically the particles of both compounds immobilised on the electrode. The CV shows only the signal of KZn[hcf]. KCu[hcc] gives no detectable signal in the mixture of both compounds as mentioned earlier. After a short time of milling and also after the first scan in CV a small reaction zone is formed, where Cu^{2+} with Zn^{2+} and [hcc] with [hcf] have a higher mobility than in the parent compounds (Fig. 11b). The presence of the new solid mixed phase can be deduced from CV and XRD. In CV, a new signal appears at a different formal potential. The position of the new voltammetric system is in agreement with the potential of the reference substance $K_{0.4}Cu_{0.65}Zn_{0.65}[hcc]_{0.55}[hcf]_{0.45}{\cdot}6\ H_2O$. The X-ray powder patterns support the diminishment of the amount of KZn[hcf] and the increase of the lattice parameters of the cubic phase by introducing larger ions. After this short time of milling, the signal of the redox system of KZn[hcf] can also be found in CV; however, it is already influenced by a new chemical environment. It can be assumed that the mixing process does not proceed with the same rate for the anions and cations. Probably, the first step is the diffusion of the cations because they are much smaller than the complex anions. Thus it is logic to assume that mixed CuZn[hcf] and CuZn[hcc] are formed leading to the rather strong shift shown in Fig. 3a. This is followed by an interdiffusion of the anions and the formation of the quaternary solid solution KCuZn[hcf][hcc]. After longer milling time or more scans in CV a decrease of the signal of the transition zone is observed. The peak currents of this signal become smaller, because a dilution of the [hcf] units by electrochemically inactive [hcc] units takes place. The position of the formal potential of this redox system is not varying very much, because substitution of the C-bound metal ion does not influence the formal potential of the low spin iron ions that much [40]. After very long time of milling one can still find small amounts of the hexagonal phase in powder diffractograms and an oxidation peak of KZn[hcf] in CV. This means that a complete mixing of both the cubic and hexagonal compound can be excluded (Fig. 11c). The crystal water was found to be necessary for the mechanochemical reaction.

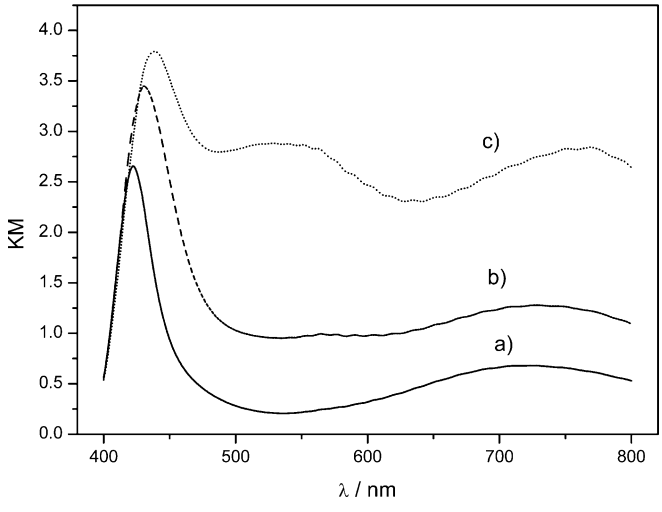

Fig. 10 Diffuse reflectance spectrum transformed into the Kubelka–Munk function of the mixture of KZn[hcf] and KCu[hcc] after **a** 1 min, **b** 25 min, **c** 2 h milling

Conclusions

This study shows that under very different conditions, i.e., in electrochemical redution/oxidation cycles and in mechanochemical experiments, two metal hexacyanometalates react to form a solid solution. The driving force must be in both cases the mixing entropy, however, the activation of the reactants is achieved differently. When the two hexacyanometalates are electrochemically cycled between the two possible oxidation states ($Cu^{2+/+}$ for KCu[hcc], and $Fe^{3+/2+}$ for KZn[hcf]) the solubilities will be also cyclically increased and decreased [51]. This may be sufficient to explain the formation of the mixed solution when the two compounds are in

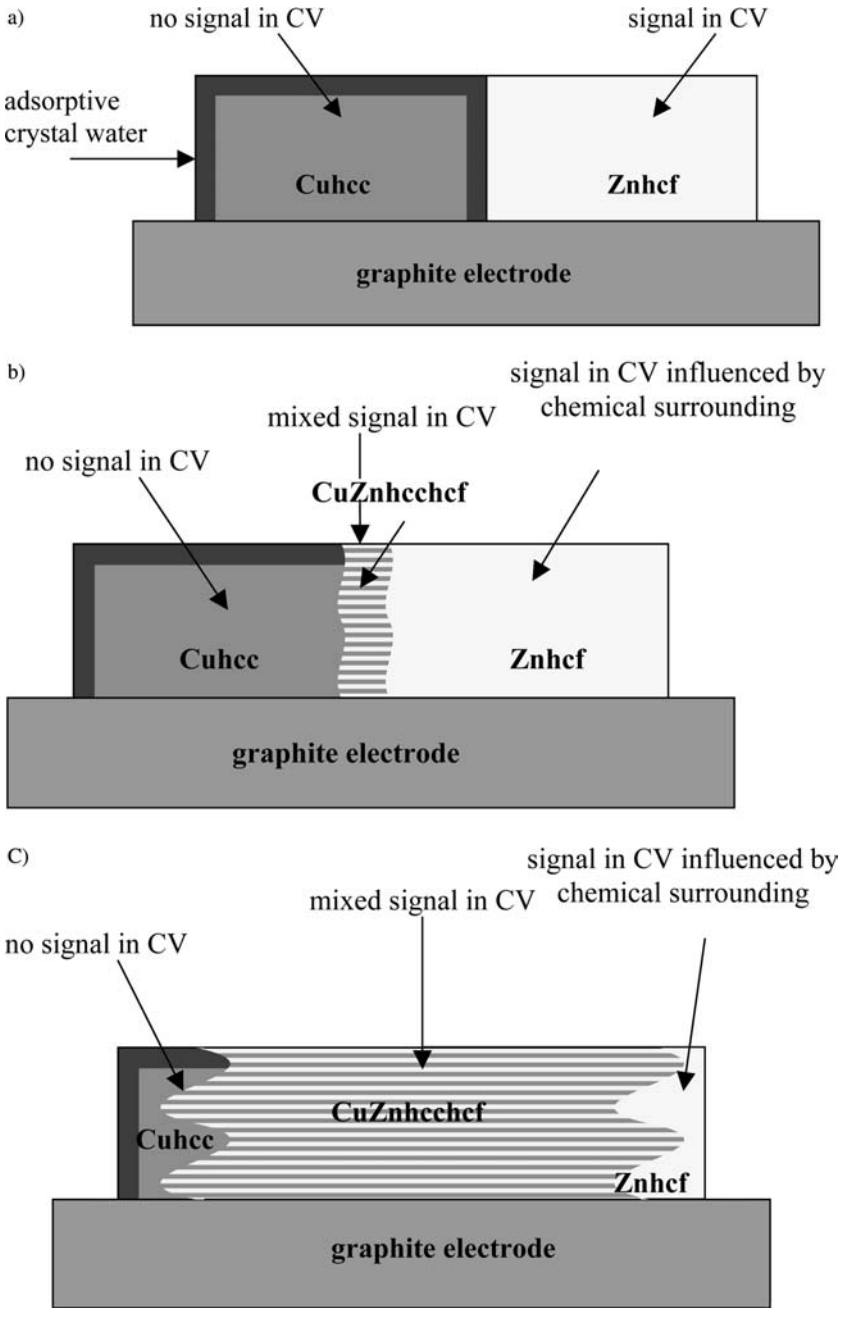

Fig. 11 Scheme of the solid state reaction between KZn[hcf] and KCu[hcc] **a** before milling, **b** after a short time of milling, **c** after a long time of milling

intimate contact on the electrode surface and redox cycled in CV experiments. The milling experiments clearly showed that a certain water content is necessary to achieve the solid solution formation. As it is well known for tribochemical reactions, it can be supposed that the mechanical energy produces the formation of a softened interphase in which the ions possess a larger diffusivity than in the intact lattices of the parent compounds. It is also known from the literature that additives leading to sorption or a reaction with the solid during milling experiments strongly influence tribochemical reactions. It is assumed that the surface energy of a solid is reduced by the influence of an additive and some of its mechanical properties are assumed to be changed. Such an effect is remarkable, i.e., for ionic crystals by the addition of polar substances like water [55]. The present study is the first example that electrochemical cycling of a powder mixture can achieve the same results as a mechanical activation by milling.

Acknowledgements The authors acknowledge substantial support by the DFG. Additional support by Fonds der Chemischen Industrie is gratefully acknowledged.

References

1. Siperko ML, Kuwana T (1987) Electrochim Acta 32:765
2. Engel D, Grabner EW (1985) Ber Bunsenges Phys Chem 89:982

3. Itaya I, Uchida I (1986) Acc Chem Res 19:162
4. Horányi G, Inzelt G, Kulesza PJ (1990) Electrochim Acta 35:811
5. Viehbeck A, DeBerry DW (1985) J Electrochem Soc 132:1369
6. Kellawi H, Rosseinsky DR (1982) Electroanal Chem 131:373
7. Itaya K, Shibayama K, Akahoshi H, Toshima S (1982) J Appl Phys 53:804
8. DeBerry DW, Viehbeck AJ (1983) Electrochem Soc 130:249
9. Mortimer RJJ (1991) Electrochem Soc 138:633
10. Greenberg CB (1994) Thin Solid Films 251:81
11. Monk PMS, Mortimer RJ, Rosseinsky DR (1995) Electrochromism: fundamentals and applications. VCH, Weinheim
12. Neff VD (1985) J Electrochem Soc 132:1382
13. Grabner EW, Kalwellis-Mohn S (1987) J Appl Electrochem 17:653
14. Kalwellis-Mohn S, Grabner EW (1989) Electrochim Acta 34:1265
15. Kuwabara K, Nunome J, Sugiyama K (1991) Solid State Ionics 48:303
16. Jayalakshmi M, Scholz F (2000) J Power Sources 91:217
17. Sinha S, Humphrey BD, Bocarsly AB (1984) Inorg Chem 23:203
18. Dong S, Che G (1991) J Electroanal Chem 315:191
19. Weißenbacher M, Kalcher K, Greschoing H, Ng W, Chan WH, Volgaropoulos A (1992) Fresenius J Anal Chem 344:87
20. Shankaran DR, Narayanan SS (1998) Bull Electrochem 14:267
21. Cola M, Ganzerli Valentini MT (1972) Inorg Nucl Chem Lett 8:5
22. Skrivastava SK, Jain CK, Oberoi CK, Sharma AK (1982) Can J Chem 60:1681
23. Mekhail FM, Benyamin K (1991) Radiochim Acta 55:95
24. Botros N, Elbayoumy S, Elgarhy M, Marei SA (1991) J Radioanal Nucl Chem Ar 147:333
25. Keggin JF, Miles FD (1936) Nature (London) 137:577
26. Ludi A, Güdel HU (1973) Struct Bonding 14:1
27. Buser HJ, Schwarzenbach D, Petter W, Ludi A (1977) Inorg Chem 16:2704
28. Kahlert H (1998) PhD Thesis. Humboldt-Universität, Berlin
29. LoosNeskovic C, Fedoroff M, Garnier E, Gravereau P (1984) Talanta 31:1133
30. LoosNeskovic C, Fedoroff M, Garnier E (1989) Talanta 36:749
31. Dostal A, Schröder U, Scholz F (1995) Inorg Chem 34:1711
32. Brown DB, Shriver DF, Schwartz LH (1968) Inorg Chem 7:77
33. Brown DB, Shriver DF (1969) Inorg Chem 8:37
34. House JE, Bailar JC (1969) Inorg Chem 8:672
35. Reddy SJ, Dostal A, Scholz F (1996) J Electroanal Chem 403:209
36. Zakharschuk NF, Nammov N, Stösser R, Schröder U, Scholz F, Mehner H (1999) J Solid State Electrochem 3:264
37. Schwudtke D, Stößer R, Scholz F (2000) Electrochem Comm 2:301
38. Kulesza PJ, Malik MA, Schmidt R, Smolinska A, Miecznikowski K, Zamponi S, Czerwinski A, Berrettoni M, Marassi R (2000) J Electroanal Chem 487:57
39. Kulesza PJ, Malik AM, Skorek J, Miecznikowski K, Zamponi S, Berrettoni M, Giorgetti M, Marassi R (1999) J Electrochem Soc 146:3757
40. Widmann A, Kahlert H, Petrovic-Prelevics I, Wulff H, Yakhmi JV, Bagkar N, Scholz F (2002) Inorg Chem 41:5706
41. Bertrán JF, Pascual JB, Hernández M, Rodríguez R (1988) React Solid 5:95
42. Scholz F, Dostal A (1995) Angew Chem Int Ed Engl 34:2685
43. Schröder U, Scholz F (2000) Inorg Chem 39:1006
44. Scholz F, Meyer B (1998) Voltammetry of solid microparticles immobilised on electrode surfaces. In: Bard A, Rubinstein I (eds) Electroanalytical chemistry, vol 20. Marcel Dekker, New York
45. Fiedler DA, Scholz F (2002) Electrochemical studies of solid compounds and materials. In: Scholz F (ed) Electroanalytical methods. Springer, Berlin Heidelberg New York
46. Scholz F, Schröder U, Gulaboski R (2005) The electrochemistry of immobilized particles and droplets. Springer, Berlin Heidelberg New York
47. Rodriguez-Carvajal J (1990) Collected abstracts of powder diffraction meeting. Toulouse, France, p 127
48. Rodriguez-Carvajal J, Roisnel T (1998) Newsletter 20:35
49. Brauer G (1954) Handbuch der präparativen anorganischen Chemie. Ferdinand Enke Verlag, Stuttgart
50. Scholz F (2002) Thermodynamics of electrochemical reactions. In: Scholz F (ed) Electroanalytical methods. Springer, Berlin Heidelberg New York
51. Bárcena Soto M, Scholz F (2002) J Electroanal Chem 512:183
52. Siebert H, Jentsch W (1981) Z Naturforsch B Anorg Chem Org Chem 36:123
53. Huhey JE, Keiter EA, Leiter RL (1995) Anorganische Chemie-Prinzipien von Struktur und Reaktivität. Walter de Gruyter, Berlin New York
54. Ayers JB, Waggoner WH (1971) J Inorg Nucl Chem 33:721
55. Heinicke G (1984) Tribochemistry. Akademie-Verlag, Berlin